Planetary Gear Series Elastic Actuation for a Compliant Exoskeleton Elbow Joint

Benjamin Jenks, Dr. Filip Stefanovic
COMAND Lab, Department of Biomedical Engineering,
University at Buffalo the State University of New York, Buffalo 14215 USA

***Abstract*— Stroke survivors often face upper limb impairment, particularly elbow movement, impacting daily activities. Traditional rehabilitation methods often fall short in addressing daily activity rehabilitation, where a patient could have on average 2.991 Nm loss in torque. Exoskeletons are one way to provide functional assistance during rehabilitation, giving patients the opportunity to perform more repetitions, and reduce fatigue. This study proposes a novel design of a compliant 3D-printed Series Elastic Actuator (SEA) device for elbow movement rehabilitation exoskeletons. The SEA design incorporates a planetary gear system and torsional spring, offering compliance, adaptability, and cost-effectiveness. Torque assessments of individual functional performance enabled us to use a 4.12 Nm motor at 26 RPM to achieve a max torque of 12.36 Nm at 8.67 RPM.. A PID ensures precise movement of the motor at 0.26º per count to align with the desired user arm position. Moreover, the design of this SEA allows for easily adjustable parameters to fit different joints, or various torque output configurations. Qualitative testing confirmed spring compliance of 18.95º and elastic element compliance of 32.43º. This study presents a new 3D printed SEA design for compliant exoskeleton joints to enhance elbow rehabilitation or other assistive robots.**

I. Introduction

Stroke, a cerebrovascular accident, remains a leading cause of disability, with 62%-88% of survivors experiencing upper limb impairment. Regaining elbow movement is crucial for daily activities such as eating, dressing, and hygiene, yet traditional rehabilitation often falls short in addressing these specific deficits [1, 2].

When rehabilitating elbow flexion and extension, there are several challenges. The elbow joint involves multiple muscles, each of which contributes to various aspects of movement (flexion, extension, pronation, and supination). Effective rehabilitation demands intensive repetitive practice of elbow movements, often unavailable due to resource constraints and patient fatigue [3]. Traditionally, therapeutic intervention can have limited effect due to deficits such as spasticity or weakness, hindering functional recovery. Thus, upper-arm assistive devices offer ways to facilitate increase use in a limb, but have their own limitations. For example, many devices lack compliant actuation, potentially causing discomfort or injury due to overly rigid interactions with the patient's limb. Moreover, the biomechanics of movement are specific to individuals, and thus having a personalizable actuation in the exoskeleton is essential for comfort and usability. Thus, tailoring interventions to individual needs is crucial for maximizing effectiveness [4].

There currently exists devices that are 3D printed exoskeletons for the assistance in rehabilitation. Two of these are the passive exoskeleton by Cristina Sanchez and team and the active exoskeleton by Manuel Vélez-Guerrero seen in Fig 1.a and b, respectively [5, 6].

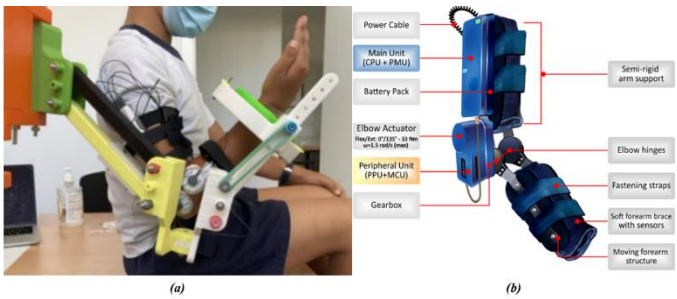

Fig. 1. (a)Passive exoskeleton by Crisitina Sanchez and team.[5] (b) Active exoskeleton by Manuel Vélez-Guerrero and team [6].

Passive exoskeletons, such as the one presented in Sanchez's study, primarily provide guidance and support rather than actively powering movement. They achieve this by incorporating features that resist unwanted motions while allowing for user-driven movement within a desired range. In this specific design, the focus is on aiding elbow flexion, not both flexion and extension [5]. Active exoskeletons, on the other hand, utilize actuators to actively assist or even drive limb movement. The design proposed by Vélez-Guerrero exemplifies this approach, featuring an autonomous and wearable system with force sensors for movement detection and assistance [6]. Traditional stationary rehabilitation devices, like those depicted in Fig 1.a, have limitations in terms of portability and user experience. This has driven research towards portable exoskeleton designs (Fig 1.b) that offer greater flexibility and can be used in various settings. However, ensuring user safety during rehabilitation remains paramount in portable designs.

This proposal seeks to address these limitations by developing a compliant 3D printed Series Elastic Actuator (SEA) device specifically designed for elbow movement rehabilitation.. The inherent elasticity of the actuator design, can provide safer and more comfortable interactions with the patient's limb. Additionally, 3D printing allows for personalized design and fabrication, allowing for rapid personalization of exoskeleton performance. Similarly, 3D printing also offers the potential for affordable device production, increasing accessibility for wider patient populations.

II. METHODS

In this section, the novel design of a 3D-printed SEA is discussed. First, the methodology for a SEA is analyzed, and the use of a planetary gear system. The calculations and torque requirements were examined for the elbow actuation.

A. Series Elastic Element

Traditionally, actuator systems suffer from inherent stiffness due to the rigid connection between the transmission (gearbox) and load. This design limits the ability of the system to adapt to varying environments and safely interact with objects. The overall system actuation has two angles of motion, θ_m, and θ_l, the motor angle and load angle, respectively. These angles are directly related to each other through the gear ratio N_m of the gearbox, as shown in Equation (1).

$$\theta_l = N_m^{-1}\theta_m \tag{1}$$

This coupling essentially reduces the system to a single degree of freedom, thereby limiting flexibility. To address this limitation, researchers like Pratt [7] proposed introducing an elastic element between the gearbox and the load seen in Fig 2.

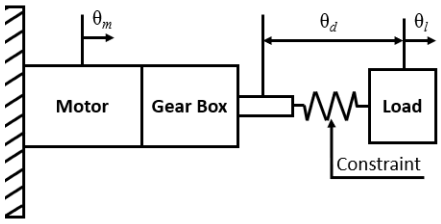

Fig. 2. Actuator with spring element between transmission and load [7].

The inclusion of the spring in a SEA configuration introduces an additional degree of freedom to the system. While there is still a single kinematic constraint, often represented by the differential mechanism seen in Equation (2), the spring allows for independent movement between the motor and the load.

$$\theta_d = N_m^{-1}\theta_m - \theta_l \tag{2}$$

Another method for creating a SEA is to use an element that has inherent elasticity, which is also seen in Pratt [5].

B. Planetary Gear

A planetary gear was introduced to achieve the differential mechanism constraints set by the SEA system. This transmission is composed of a sun gear, planet gears, a ring gear, and a carrier. The planet gears are connected to the carrier which makes the planetary gear an epicyclic gear seen in Fig 3.

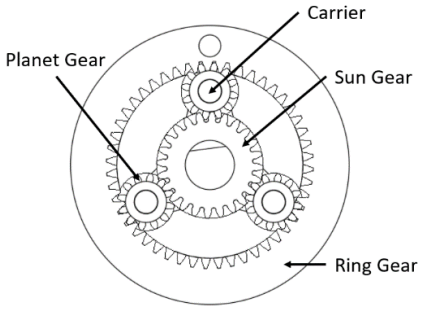

Fig. 3. Planetary gear schematic.

The sun gear, through the input shaft, observes the input torque from the source, such as a motor. Planet gears with a carrier connect the sun and the ring gears. The torque output can be determined based on the fixed element in the planetary gear. With the ring gear fixed the transmission ratio (i_r) becomes

$$i_r = 1 + \frac{N_r}{N_s} \tag{3}$$

where N_r and N_s are the numbers of teeth on the ring gear and sun gear, respectively. From this, the torque can be found using

$$\tau_c + i_r\tau_s = 0 \tag{4}$$

where τ_c and τ_s are the carrier and sun gear torques, respectively.

The use of a planetary gear allows for compactness, high efficiency, and low backlash. These qualities render planetary gears ideal for SEA-based rehabilitation devices. This combination allows for safer and more refined movement control in patients undergoing therapy.

C. Torque Assessment

We calculated elbow torque in order to determine equipment needed for appropriate levels of actuation. To do this, typical torque at the elbow in healthy and post-stroke individuals were calculated. Since many post-stroke patients have a large variability in body segment usability, weight, mass, and length, the amount of torque applied at the elbow can also vary [8].

1) Human Properties

The calculation of elbow torque in healthy and post-stroke individuals was completed using body segments lengths as measured by Harless, and reported by Drillis [9].

TABLE I. REPORTED AVERAGE BODY SEGMENT MEASUREMENTS

	Average Body Segment Values	
	Length (cm)	***Weight (g)***
Hand	20.3	540
Forearm	29.9	1160
Upper Arm	36.3	2070

Patients with impaired motor function often experience a decrease in both movement speed and joint strength (torque) of the affected limbs. Research suggests average torque reduction after a stroke of 63% in elbow extension strength [10]. This is

used to approximate the torque assistance needed by an elbow exoskeleton. By incorporating these torque loss values into the calculations, a more realistic model of the elbow joint function can be created.

The patient's center of mass (COM) also plays a vital role in determining the torque generated at the elbow. The distance between the COM and the elbow joint influences the effect of gravity on the forearm and hand. The data in Table II. (as reported in [11]) provide the average COM values for males and females, which were used for further calculations.

TABLE II. PERCENTAGE OF CENTER OF MASS

	COM (%)		
	Male	***Female***	***Average***
Hand	79.00	74.74	76.87
Forearm	45.74	45.59	45.67
Upper Arm	57.72	57.54	57.63

Muscles exert force on bones through their insertion points, which are the locations where the muscles and tendons attach. These insertion points define the spatial location of the forces acting on the forearm during the flexion and extension movements. In addition, a typical moment arm value of 2.5 cm, as reported in [12], was used to represent the average muscle insertion points across different arm positions.

2) Torque Calculations

To best evaluate the forces acting on the body in this scenario, a free-body diagram was used to represent the forces. In this case, we focus on the forces affecting the forearm during elbow flexion and extension. The diagram uses letters to represent different body parts: shoulder (S), elbow (E), wrist (W), and hand (H).

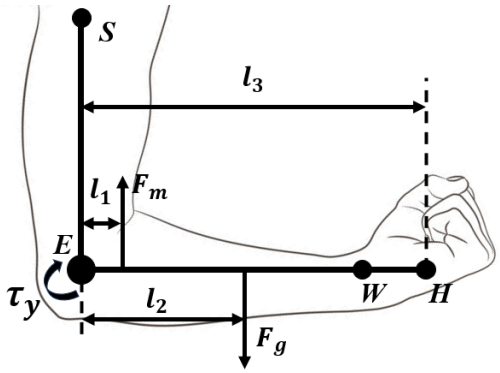

Fig. 4. Free-body diagram used to calculate the torque about the elbow.

The following key lengths and forces are also depicted:

l_1: Length of the muscle insertion point
l_2: Distance of the center of mass from the elbow joint
l_3: The total length of the forearm
F_m: The force of the flexion/extension exerted by muscles
F_g: Force of gravity
τ_y: Uniaxial torque about the elbow

The center of mass (COM) of the forearm can be calculated using Equation (5). Where m_1 and m_2 represent the mass of the forearm and hand, respectively. Then x_1 and x_2 represent the distances of the forearm and hand COMs from the elbow joint, respectively.

$$COM = \frac{m_1 x_1 + m_2 x_2}{m_1 + m_2} \tag{5}$$

Anatomical proportionality was used to determine lengths x_1 and x_2, from a previous study [11]. It is known that 45.665% and 76.87% are the percentages of the total length of the arm to the COM for the forearm and hand from the elbow joint, respectively. Using these percentages and the average forearm length data from another study [9] (adjusted for gender), the COM was calculated for the entire forearm.

The free-body diagram allows us to derive an equation for analyzing the forces acting on the forearm.

$$\sum \tau_y = F_m l_1 - F_g l_2 = 0 \tag{6}$$

$$F_m = \frac{F_g l_2}{l_1} \tag{7}$$

$$\tau_y = F_m l_1 \tag{8}$$

From Equation (7), the force exerted by the muscles can be determined, and this is substituted into Equation (8) to obtain the total torque produced about the elbow.

3) Torque Results

A mass of 35 g was added to the forearm to obtain the most accurate torque for the elbow. This was added to account for the mass of the exoskeleton, affecting the torque. To determine the amount of torque required to assist the user the percentages reported in [10] were used.

$$\tau_{lost} = 0.63\tau_y \tag{9}$$

Using Equations 5-9 the following results were obtained:

TABLE III. RESULTS AND VALUES FOR THE LENGTH, COM, FORCE, AND TORQUE

Variable	Value
l_1	2.5 cm
l_2	27.89 cm
l_3	50.2 cm
x_1	22.9 cm
x_2	38.6 cm
F_m	189.88 N
τ_y	4.747 Nm
τ_{lost}	2.991 Nm

III. Results

Based on the principles and parameters stated previously, the following design was created. The process for creating the model and the hardware used are also discussed.

A. DC Motor Selection

An electric motor must provide sufficient assistive torque during human movements to counteract the torque loss in forearm motor impairment. Thus, it is important to consider the characteristics of human motion when selecting a motor for this purpose. Therefore, we focused on maximum torque and angular velocity when selecting a motor for our design. We also encountered size limitations, whereby the motor needed to not exceed 40 mm from the arm to limit bulkiness.

The motor, along with the series elastic element, had to be able to provide smooth movement that worked bi-directionally to align with the natural movement of the elbow. We also selected a motor with a built-in encoder for feedback, along with a motor controller. Hence, we used a 12V, 26 RPM motor (638242, RobotZone, USA) with a stall torque of 4.12 Nm was selected [13]. The motor controller was a SparkFun Motor Driver (14450, SparkFun, USA) [14].

Fig. 5. 12V planetary geared motor with encoder.

This motor does not require additional drivetrains in order to achieve the desired torque of 2.991 Nm, as per Equation (8). This means that the selected motor with our added planetary gear system to the shaft of the motor providing a larger range of providable torque. The desired torque calculations were calculated using averages meaning there will be cases where a greater torque is needed.. The motor rotation speed of 26 RPM also allows for a larger range of speeds for the users, since it converts to an elbow rotation rate of 0 °/s to 52 °/s. This rotational speed is based on the speed on the forearm after the planetary gear reduction. The addition of the encoder to the motor also allows for the motor shaft to align with the movement of the user's arm. This was paired with a motor driver to allow the motor to operate in the bi-directional movement previously mentioned.

B. Elastic Element

A SEA is defined by the elasticity experienced during actuation. This allows the SEA to absorb impact forces and release stored energy back to the output. The core principle of SEAs relies on the use of series elasticity, which follows Hooke's Law. This ensures the linear behavior of elastic materials, enabling precise force control relative to the position of the actuator. While novel elastic materials, air compression or magnetic forces are being researched, mechanical springs remain the most common choice owing to their widespread availability, affordability, and variety of commercially available options. Here, we implement our SEA using torsional elasticity on a planetary gear system. Thus, a torsional spring was chosen. The spring operates within a range of ±2.109 Nm and is assumed to exhibit good linearity regardless of the direction of rotation.

The spring in our SEA has two roles as both a torque sensor and torque generator. Therefore, the performance of the SEA is heavily influenced by the characteristics of the spring. It can be observed that the SEA's maximum torque is directly linked to the stiffness of the spring. However, there is a trade-off between the two. If the spring is too stiff, excessive torque can be generated, leading to user discomfort during the rehabilitation exercise. The design of the spring must be carefully considered to achieve the best balance between maximum torque and precise motor control. This ensures a comfortable and effective user experience.

The mechanical design of the torsional spring used in the SEA can be seen illustrated in Fig 6. [15]. The spring constant, a measure of stiffness, is determined by the spring's geometry (diameter D, wire diameter d, and number of coils N) and the material's elastic modulus. The specific values for these parameters are provided in Table 1.

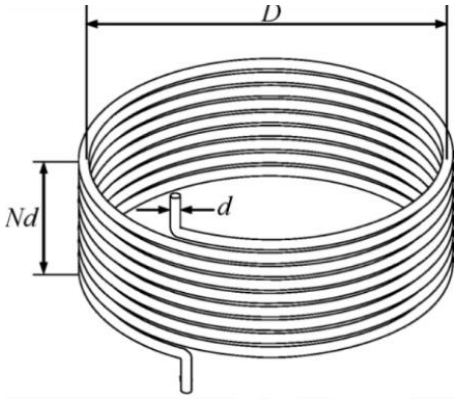

Fig. 6. Torsional spring design.

TABLE IV. Torsional Spring Specifications

Specification	Value
Desired max deflection	±20 degrees
Desired max torque	±3 Nm
Spring diameter *D*	29.032 mm
Wire diameter *d*	2.667 mm
Number of turns *N*	7
Spring constant *k*	0.015 Nm/deg

C. Operating Design Principle

The planetary gear system, described in Sec. II-B had three parts that rotated relative to the fixed ground. The chosen configuration utilizes the sun gear as the input and the carrier as the output to achieve a high gear ratio. The elasticity of the system utilizes a torsional spring between the ring gear and

ground (fixed motor bracket). This includes the motor stator being fixed to the motor bracket and the rotor being connected to the sun gear. The design employed the DC motor described in Sec. III-A, which has a speed of 26 RPM speed and 4.12 Nm of max torque for the 2.991 Nm loss torque by the user. The integration of the motor into the system and the component breakdown of the system are shown in Fig. 7.

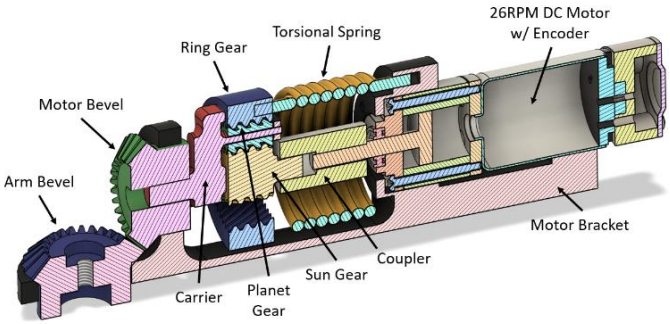

Fig. 7. Cross-sectional diagram of the proposed torsional spring SEA device.

The torque produced by the motor becomes the input torque for the planetary gear system by connecting the motor rotor to the sun gear, ultimately driving the entire actuator system. The sun gear position is then related to the angular position of the motor rotor and is measured by the encoder on the motor. The carrier of the system serves as the output shaft, which connects to the load being moved. The operating principles are shown in Fig. 8.a.

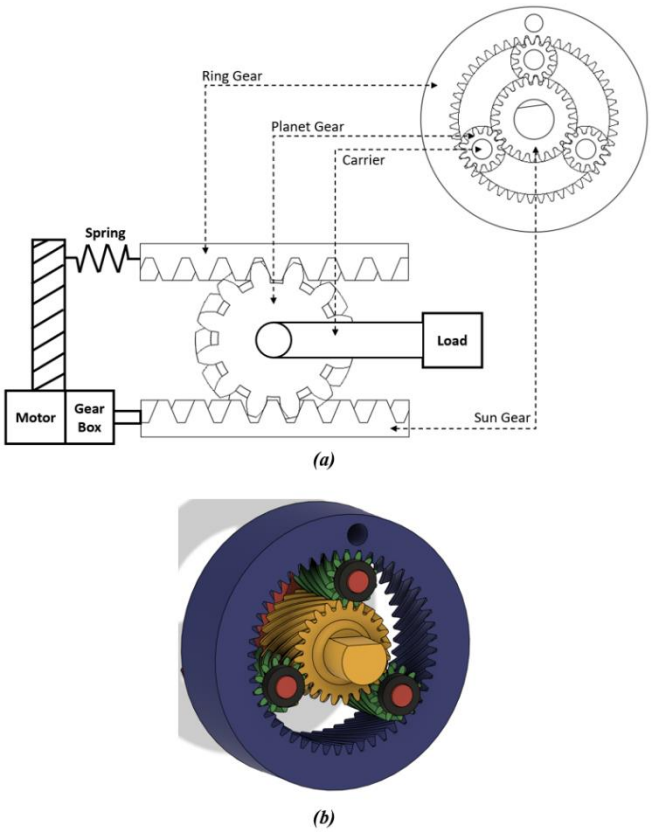

Fig. 8. (a) Rotary-to-linear motion projection schematic of the planetary SEA system. (b) Helical gears used in the planetary gear system.

This illustrates the relative motions of the three key components in the actuator: ring gear (spring system), sun gear (motor system), and carrier (load system) [16]. It is important to note that this figure depicts a planetary gear system with a cutaway view. This shows the motions of the sun and ring gear projected as linear motions for easier visualization.

D. Software Control

To control the device, two different scripts were written, where one controlled the device when using the torsional spring design and the other when using the elastic element design (Appendix A). Both scripts were written in C++ and uploaded to an Arduino using the PlatformIO IDE. For both scripts, the code utilizes a proportional-integral-derivative (PID) controller to control the motor position. This is achieved by continuously reading the encoder value that is received by the Arduino and then computing a control signal based on the difference between the current and target positions of the device. The two scripts utilize different target positions based on testing to identify ideal encoder positions based on the position of the user's arm. For this to be accurate, the scripts assume the position of the arm to be at a 70º angle (Fig. 9.a). to start and end at 180º (Fig. 9.b) and return.

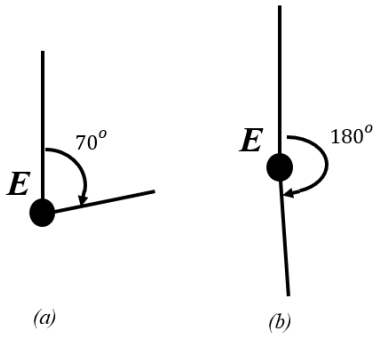

Fig. 9. Arm position during rehabilitation: (a) start and (b) full extension positions.

The amount of accuracy that could be achieved by the encoder was found based on the encoder's specifications. It was found that the encoder could achieve 0.26º per PID count. This was calculated from the amount of pulse cycles from the encoder per revolution of the motor shaft and the internal motor gear ratio. The PID was tuned by testing the position of the encoder against the desired target position and adjusting the PID components to achieve a critically damped system. This was achieved to ensure that no injury would occur to the user by going past the desired location and maintaining the movement at a consistent speed. All scripts are available on our public repository (COMAND Lab/SEA Exoskeleton).

E. Final Model

1) Torsional Spring Design

The torsional spring SEA design followed the previously discussed principles. The process of creating the final model is discussed in the following section (Sec. IV) with reasoning for specific design choices. The full model design, shown in Fig. 10.a. shows the full rehabilitation device. This design utilized PLA plastic to print all components except for the motor and

spring element to reduce the weight and material cost of the device.

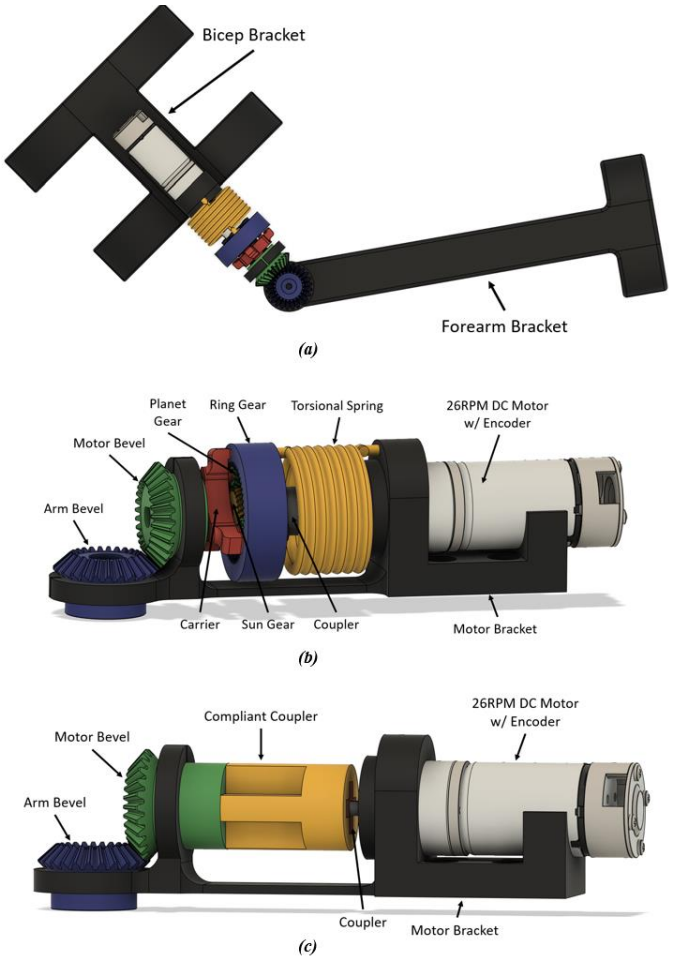

Fig. 10. (a)Full-model design of the proposed torsional spring SEA device. (b) Component view of proposed torsional spring SEA actuator. (c) Component view of the proposed elastic element actuator.

This device utilizes the components shown in Fig. 7., where the section view identifies the components required to understand the operating principles. This design also utilized two brackets to connect the actuating device to the user using Velcro straps. Figure 10. b shows the non-sectioned view of the components for the proposed SEA actuator system.

In the proposed design, a 3:1 helical planetary gear system was chosen. With a 3:1 gear ratio for the planetary gear system, using Equation 4., the max output torque of the system can be found to be 12.36 Nm. A 3:1 ratio could be achieved by using a gear tooth ratio of 12:24:48 as the planet, sun, and ring gear, respectively. With a maximum output torque of 12.36 Nm, the system can be used for a larger population of users. The bevel gears used in the actuator system were maintained at a 1:1 gear ratio to maintain the output torque seen by the user at 12.36 Nm maximum.

A stress test was conducted to quantify the compliance of the device within the anticipated range of motion under un-powered conditions. This test isolated the contributions of the spring mechanism and the planetary gear system. The bicep bracket was secured, and the forearm bracket was initially positioned at 180º. This position served as the baseline. The forearm bracket was then rotated until the spring became engaged and due to the fixed sun gear (motor inactive). The angle between the initial and engaged positions were measured, quantifying the system compliance at 34.38º. To isolate the contribution of the planetary gear system, a secondary test was performed by mimicking the initial conditions of the stress test, but stopping the rotation before the spring engaged. This measurement, 15.43º, represented the inherent compliance of the planetary gear system. By subtracting this value from the total compliance measured in the first test, the contribution of the spring mechanism was determined to be 18.95º.

2) Compliant Connector Design

The compliant element design of the proposed device used the principles described in Pratt [7]. This method utilizes the inherent elasticity of the material. For this design, TPU was used as the elastic material because of its highly elastic nature. This design does not use the previously discussed planetary gear system, which only allows the maximum torque output to the original 4.12 Nm that the motor can provide. In this design, there is not as large a torque distribution for users, but it still allows for the average torque needed based on the calculated torque loss in Equation 9 and is reported in Table III. Figure 10.c shows the component view with the elastic element introduced.

As previously stated, TPU was used to make the elastic element labeled as a compliant coupler. The compliant coupler consists of two materials. Due to the inherent elasticity of TPU, a portion of the coupler was made using PETG to have rigidity through the process of a multi-material print.

The same testing methods were performed for the compliant coupler to determine the amount of compliance achieved by the TPU element as done with the torsional spring design. In this testing there was no compliance seen by the planetary gear system because this did not exist for this design. Thus, when calculating the compliance, the measurement of 32.43º seen was from the compliant coupler.

IV. Fabrication

Previously, the mechanical and dynamic principles were discussed to create the proposed design. The following section discusses the process and iterations used to create the design. The specific properties of the design are also discussed. All models were designed in Fusion360 and printed using a Robo R2 and Prusa MK3 3D printer. Design drawings can be seen in Appendix B.

A. Torsional Spring SEA Device

1) Bracket Design

For the first iteration of the design, the attachment of the SEA device to the user was the first element considered. This was considered for the forearm and bicep brackets. The original forearm design had a cuff that went around the forearm-wrist area with a small amount of room to slide the wrist through (Fig. 11.a). In the original design, use by multiple individuals was not considered.

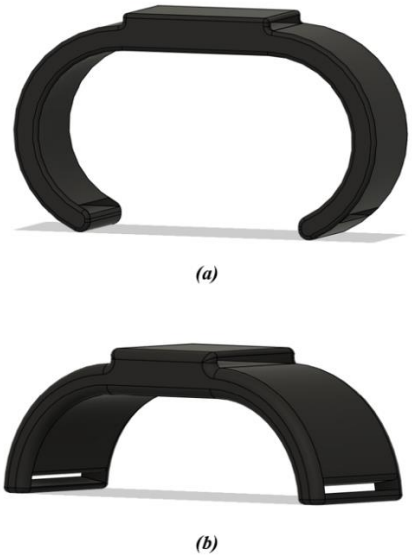

Fig. 11. (a) Original cuff design (b) Final cuff design

To allow the device to be used for more individuals, the wrist cuff was expanded by enlarging the opening for the wrist to fit into and ensure that the cuff did not wrap around the wrist as drastically (Fig 11.b).

The bicep bracket had been considered for multiple users when designing the cuff. To reduce the possibility of irritation and to allow more users to use the device seamlessly, the bicep bracket was designed to have a length 95 mm order to minimize rubbing against body parts. Both attachment brackets were built with the ability of Velcro holes to attach the device to the user.

2) Motor Bracket

In this design, the weights of the components were designed to prevent slipping of the motor bevel gear. To combat the slippage of the motor and arm bevel gears, a brace was added to prevent the gears from slipping (Fig. 12.a).

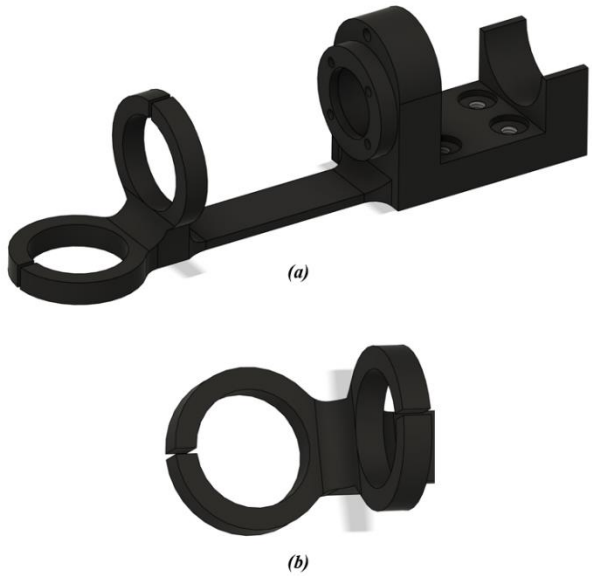

Fig. 12. (a) Motor bracket with brace. (b) Brace with sections removed for gear placement.

Both gear locations were built with a missing section to allow for proper assembly of the gears. Without these sections, the gears would not be able to be placed in their respective locations, because the other gear would be in the way (Fig. 12.b). There would also be some flexibility in the PLA that allows the gears to be placed in the brace.

3) Planetary Gear

The planetary gear design began as a spur gear system. In this system, the gears transmit rotational motion and torque between parallel shafts. The teeth of the gear come into contact at a single moment and transfer the applied force. While operating the device, it was found that when a load was applied to the output of the planetary gear system instead of transferring that load, the gears slipped. To eliminate slippage of the teeth when a load was applied, a helical gear system was introduced (Fig. 8.b). In this system, the teeth gradually engage, resulting in smoother meshing compared with spur gears. The helical gear teeth meshing also allows for a higher load capacity without tooth wear, due to the large effective contact area. Planet stops were also added as shown in black in Fig. 8.b, to stop the thrust of the planet gears.

4) Printing

To print the final design of the proposed device different settings were used to achieve the final print of the components. PLA was used to print all components. The main difference was the amount of infill used by the printing software to fill the parts. In this process, the percentage of infill is the amount of plastic used inside the part compared to air. Table V shows these values. The number of perimeters that was used to create the components was 3 for all parts. This perimeter creates the main structure and determines the strength of the part.

TABLE V. COMPONENT INFIL PERCENTAGES

Components	Infill (%)
Bicep, Forearm, Motor Brackets	30
Sun Gear, Ring Gear, Motor Bevel, Arm Bevel	60
Coupler, Carrier, Planet Gear, Planet Stops	100

B. Compliant Connector Device

For this design, multi-material printing was performed to create a compliant connecting element The total length of the complaint arm is 38 mm. The compliant arm device works by using the materials inherent elastic behaviors. To ensure the there was no separation between the two materials in a high shear force location the lengths of the materials were adjusted. Thus, the PETG section was designed to be 9.6 mm in length (orange in Fig. 13.), while the TPU was 28.4 mm in length (yellow in Fig. 13.). These lengths were chosen based on the layer height (0.2 mm) during the 3D printing process. The length also took into consideration the coupler that was in the PETG portion of the elastic element.

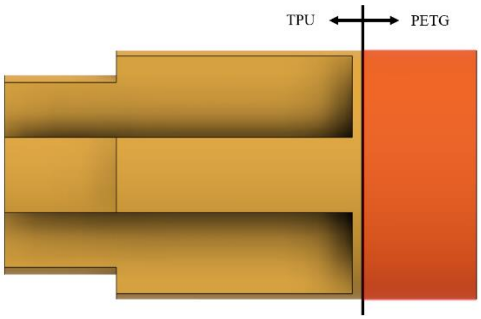

Fig. 13. Elastic element

For the PETG portion of the print, the perimeter was left at the default of 2 perimeters, with an infill of 20%. For the TPU, the perimeters were set to 12. This was done to ensure that the layers adhered well together. In addition, there was an inherent 10% overlap of the perimeter layers, creating a stronger bond, which created a greater strength against the torsional forces against the layer adhesion. TPU is a filament that has to be printed slower due to its inherent elasticity. To account for this, a 12.5% decrease in speed from the default PETG speed (45 mm/s) was used. Because the motor rotor is also very small in size (4 mm) and more compliant than the rigid PLA, a coupler was added to the motor rotor to convert the torque from the motor to the compliant arm (Fig 10.c). All other components were printed in the same manner as in the torsional spring design.

V. Discussion

This study demonstrates a planetary geared SEA design for an elbow exoskeleton. This device was designed with the ability to have compliance from the planetary geared SEA system to allow for comfort and safety during forearm flexion and extension.. This was done with a lightweight and low-cost device in mind, where the total weight of plastic and cost can be seen in Table VI.

TABLE VI. Exoskeleton Cost Analysis

Components	Plastic	Grams (g)	Cost per Gram ($)	Total Cost ($)
Torsional Spring Design	PLA	132.25	0.025	3.31
Elastic Element Design	PLA TPU PETG	122.82 6.33 2.47	0.025 0.11 0.022	3.82

With the cost of material calculated, the total cost for the device could be calculated to be $75.69 and $58.97 for the torsional spring design and the elastic element design, respectively. This shows that the desired design is low cost.

Positional control of the device based on the designed software was realized through qualitative verse quantitative observation testing. This was achieved through the use of a planetary geared motor with a speed of 26 RPM and output torque of 4.12 Nm. The position was seen through the encoder with an accuracy of 0.26º per PID count. The motor torque was then transmitted through the designed 3:1 helical planetary gear. This multiplied the torque output, making it suitable for a wider range of users. With the addition of a torsional spring, the device was observed to achieve a total compliance of 34.38º and spring compliance of 18.95º to allow user comfort and safety. The design also explored the design of a compliant connector element made of TPU as an alternative actuation method. This eliminates the planetary geared system and relies on the inherent elasticity of the TPU to provide the compliance of up to 32.43º. Further testing should be completed, where a sensor is attached to the forearm to read the angular position of the forearm and perform another PID analysis to allow for a closed-loop positioning of the forearm based on the target angle. This would also allow for the torque control of the motor to achieve the desired location if more resistance is being applied.

This device has the potential to be adapted into a wearable exoskeleton to aid users in daily activities. First, electromyography (EMG) sensors would be integrated to detect elbow flexion/extension and user intent. Machine learning algorithms would then interpret user intent and determine the appropriate exoskeleton movement to assist. Third, a position sensor would be incorporated to compare user forearm position with motor encoder readings. Finally, a larger motor could be incorporated to provide increased torque and assist with daily tasks. The desired torque can be calculated using Equations 6- 9 and considering the weight held by the user. These modifications would necessitate more rigorous testing due to the added system complexity. The current qualitative testing validates the core design principles.

VI. Conclusion

This study successfully designed and developed a 3D-printed planetary gear Series Elastic Actuator (SEA) exoskeleton for elbow rehabilitation. The proposed designs address the limitations of inherent stiffness in traditional actuator systems by incorporating a torsional spring or elastic element, thereby creating a safe and adaptable device for users with impaired elbow flexion and extension. The key achievements of this work are the design and fabrication of a low-cost and adaptable 3D-printed SEA exoskeleton as well as demonstrating the device's ability to achieve a compliance of 18.95º and 342.43º for user safety.

Future work suggests further testing with the introduction of multiple sensors to achieve more precise positioning and torque control. Additionally, the adaptation to achieve daily activity assistance by incorporating machine learning for user intent recognition, EMG sensors, and a higher-torque motor. This, study presents a promising design for a 3D-printed SEA exoskeleton with the potential to improve elbow rehabilitation and eventually transition to user assistance in everyday activities.

Acknowledgment

We would like to thank Michael Govoni (University at Buffalo, MAE Department) for providing insight and assistance in the process of multi-material 3D printing.

References

[1] C. M. Stinear, C. E. Lang, S. Zeiler, and W. D. Byblow, "Advances and challenges in stroke

rehabilitation," *Lancet Neurol*, vol. 19, no. 4, pp. 348-360, Apr, 2020.

[2] P. Langhorne, J. Bernhardt, and G. Kwakkel, "Stroke rehabilitation," *Lancet*, vol. 377, no. 9778, pp. 1693-702, May 14, 2011.

[3] K. Kawahira, M. Shimodozono, S. Etoh, K. Kamada, T. Noma, and N. Tanaka, "Effects of intensive repetition of a new facilitation technique on motor functional recovery of the hemiplegic upper limb and hand," *Brain Injury*, vol. 24, no. 10, pp. 1202-1213, 2010.

[4] G. Kwakkel, J. M. Veerbeek, E. E. van Wegen, and S. L. Wolf, "Constraint-induced movement therapy after stroke," *Lancet Neurol*, vol. 14, no. 2, pp. 224-34, Feb, 2015.

[5] C. Sanchez, L. Blanco, C. Del Río, E. Urendes, V. Costa, and R. Raya, "A 3D-printed passive exoskeleton for upper limb assistance in children with motor disorders: proof of concept through an electromyography-based assessment," *PeerJ*, vol. 11, pp. e15095, 2023.

[6] M. A. Vélez-Guerrero, M. Callejas-Cuervo, and S. Mazzoleni, "Design, Development, and Testing of an Intelligent Wearable Robotic Exoskeleton Prototype for Upper Limb Rehabilitation," *Sensors (Basel, Switzerland)*, vol. 21, no. 16, pp. 5411, 2021.

[7] G. A. Pratt, and M. M. Williamson, "Series elastic actuators."

[8] L. Van Dokkum, I. Hauret, D. Mottet, J. Froger, J. Métrot, and I. Laffont, "The Contribution of Kinematics in the Assessment of Upper Limb Motor Recovery Early After Stroke," *Neurorehabilitation and Neural Repair*, vol. 28, no. 1, pp. 4-12, 2014.

[9] R. Drillis, and R. Contini, "Body segment parameters," *Artificial limbs*, vol. 8, no. 1, pp. 44-66.

[10] P. S. Lum, C. Patten, D. Kothari, and R. Yap, "Effects of velocity on maximal torque production in poststroke hemiparesis," *Muscle & Nerve*, vol. 30, no. 6, pp. 732-742, 2004.

[11] M. Adolphe, J. Clerval, Z. Kirchof, R. Lacombe-Delpech, and B. Zagrodny, "Center of mass of human's body segments," *Mechanics and Mechanical Engineering*, vol. 21, 2017.

[12] H. Moritomo, T. Murase, S. Arimitsu, K. Oka, H. Yoshikawa, and K. Sugamoto, "The in vivo isometric point of the lateral ligament of the elbow," *The Journal of bone and joint surgery. American volume*, vol. 89 9, pp. 2011-7, 2007.

[13] Servocity. "26 RPM Premium Planetary Gear Motor w/Encoder," https://www.servocity.com/26-rpm-premium-planetary-gear-motor-w-encoder/.

[14] SparkFun, "SparkFun Motor Driver - Dual TB6612FNG (with Headers)," https://www.sparkfun.com/products/14450, 2024.

[15] A. Spring. "RH Torsional Spring," https://www.acxesspring.com/english/pt105-1248-7000-sst-rh-3500-n-in.htmlhttps://www.mwcomponents.com/shop/to-5246rscs.

[16] C. Lee, and S. Oh, *Configuration and performance analysis of a compact planetary geared Elastic Actuator*, 2016.

APPENDIX A

TORSIONAL SPRING DESIGN C++ PROGRAM

```
#include <Arduino.h>
#include <util/atomic.h>

#define ENCODER_A 2 // 5th gray wire of Motor
#define ENCODER_B 3 // 2nd gray wire of Motor
#define PWM 9 //PWM on Motor driver
#define AI1 8 // AI1 on Motor driver
#define AI2 7 // AI2 on Motor driver

void readEncoder();
void setMotor(int dir, int speed, int pwm, int in1, int in2);

volatile int position = 0;
volatile int target =1250;
long prevT = 0;
float eprev = 0;
float eint = 0;

void setup() {

Serial.begin(9600);
pinMode(ENCODER_A, INPUT);
pinMode(ENCODER_B, INPUT);
attachInterrupt(digitalPinToInterrupt(ENCODER_A), readEncoder, RISING);

pinMode(PWM, OUTPUT);
pinMode(AI1, OUTPUT);
pinMode(AI2, OUTPUT);
}

void loop() {

  ATOMIC_BLOCK(ATOMIC_RESTORESTATE) {
    if (position >= 1250) {
      target = 0;
    }
  }

  // PID Constants
  float Kp = 8;
  float Kd = 0.05;
  float Ki = 0.0;

  long currT = millis();
  float dt = float(currT - prevT) / 1000.0;
  prevT = currT;

  int pos = 0;
  ATOMIC_BLOCK(ATOMIC_RESTORESTATE) {
    pos = position;
  }

```

```
  int e = pos - target;
  float dedt = (e - eprev) / dt;
  eint += e * dt;

  float u = Kp * e + Kd * dedt + Ki * eint;

  float pwr =fabs(u);
  if (pwr > 255) {
    pwr = 255;
  }

  int dir = 1;
  if (u < 0) {
    dir = -1;
  }

  setMotor(dir, pwr, PWM, AI1, AI2);

  eprev = e;

  Serial.print("Pos: ");
  Serial.println(pos);
  Serial.print("Target: ");
  Serial.println(target);
  Serial.flush();
}

void setMotor(int dir, int speed, int pwm, int in1, int in2) {
  analogWrite(pwm, speed);
  if (dir == 1) {
    digitalWrite(in1, HIGH);
    digitalWrite(in2, LOW);
  } else if (dir == -1) {
    digitalWrite(in1, LOW);
    digitalWrite(in2, HIGH);
  } else {
    digitalWrite(in1, LOW);
    digitalWrite(in2, LOW);
  }
  analogWrite(pwm, speed);
}

void readEncoder() {
  int b = digitalRead(ENCODER_B);
  if (b > 0) {
    position++;
  } else {
    position--;
  }
}
```

ELASTIC ELEMENT DESIGN C++ PROGRAM

```cpp
#include <Arduino.h>
#include <util/atomic.h>

#define ENCODER_A 2 // 5th gray wire of Motor
#define ENCODER_B 3 // 2nd gray wire of Motor
#define PWM 9 //PWM on Motor driver
#define AI1 8 // AI1 on Motor driver
#define AI2 7 // AI2 on Motor driver

void readEncoder();
void setMotor(int dir, int speed, int pwm, int in1, int in2);

int val = 450;

volatile int position = 0;
volatile int target = val;
long prevT = 0;
float eprev = 0;
float eint = 0;

void setup() {

Serial.begin(9600);
pinMode(ENCODER_A, INPUT);
pinMode(ENCODER_B, INPUT);
attachInterrupt(digitalPinToInterrupt(ENCODER_A), readEncoder, RISING);

pinMode(PWM, OUTPUT);
pinMode(AI1, OUTPUT);
pinMode(AI2, OUTPUT);
}

void loop() {

  ATOMIC_BLOCK(ATOMIC_RESTORESTATE) {
    if (position >= val) {
      target = 0;
    }
  }

  // PID Constants
  float Kp = 8;
  float Kd = 0.05;
  float Ki = 0.0;

  long currT = millis();
  float dt = float(currT - prevT) / 1000.0;
  prevT = currT;

  int pos = 0;
  ATOMIC_BLOCK(ATOMIC_RESTORESTATE) {
    pos = position;}
```

```
53
54    int e = pos - target;
55    float dedt = (e - eprev) / dt;
56    eint += e * dt;
57
58    float u = Kp * e + Kd * dedt + Ki * eint;
59
60    float pwr =fabs(u);
61    if (pwr > 255) {
62      pwr = 255;
63    }
64
65    int dir = 1;
66    if (u < 0) {
67      dir = -1;
68    }
69
70    setMotor(dir, pwr, PWM, AI1, AI2);
71
72    eprev = e;
73
74    Serial.print("Pos: ");
75    Serial.println(pos);
76    Serial.print("Target: ");
77    Serial.println(target);
78    Serial.flush();
79  }
80
81  void setMotor(int dir, int speed, int pwm, int in1, int in2) {
82    analogWrite(pwm, speed);
83    if (dir == 1) {
84      digitalWrite(in1, HIGH);
85      digitalWrite(in2, LOW);
86    } else if (dir == -1) {
87      digitalWrite(in1, LOW);
88      digitalWrite(in2, HIGH);
89    } else {
90      digitalWrite(in1, LOW);
91      digitalWrite(in2, LOW);
92    }
93    analogWrite(pwm, speed);
94  }
95
96  void readEncoder() {
97    int b = digitalRead(ENCODER_B);
98    if (b > 0) {
99      position++;
100   } else {
101     position--;
102   }
103 }
```

APPENDIX B:

ARM BEVELSCHEMATIC

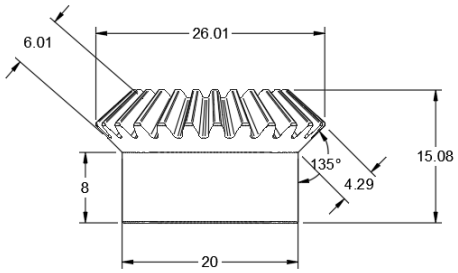

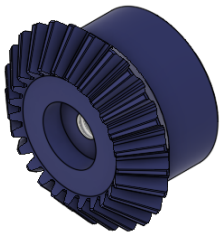

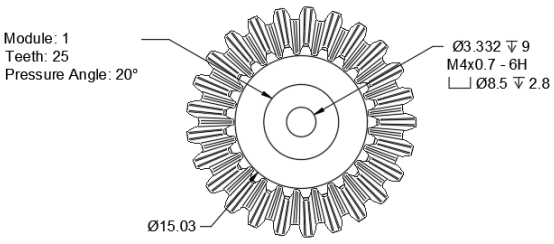

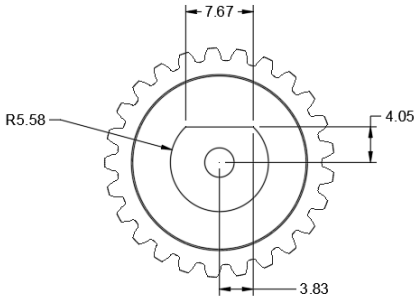

DIMENSIONS ARE IN MM TOLERANCE: ± 0.025 MM	PROJECT SEA Elbow Exoskeleton			
	TITLE Arm Bevel			
APPROVED	SIZE B	CODE	DWG NO Arm_Bevel_V6	REV 6
CHECKED				
DRAWN Benjamin Jenks 4/12/2024	SCALE 2.5:1	WEIGHT	SHEET 1/1	

BICEP SCHEMATIC

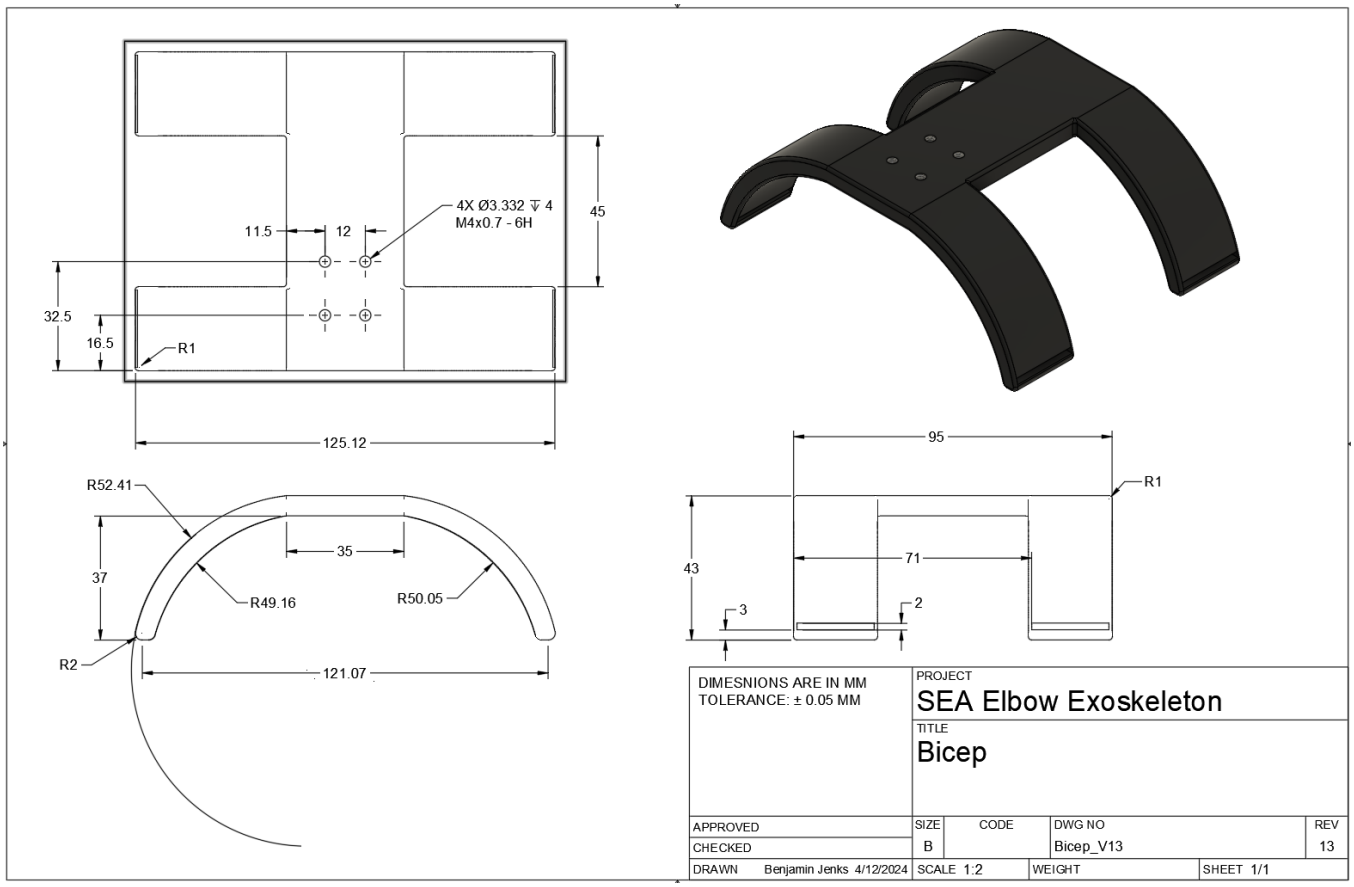

DIMESNIONS ARE IN MM TOLERANCE: ± 0.05 MM	PROJECT: SEA Elbow Exoskeleton			
	TITLE: Bicep			
APPROVED	SIZE: B	CODE	DWG NO: Bicep_V13	REV: 13
CHECKED				
DRAWN: Benjamin Jenks 4/12/2024	SCALE: 1:2	WEIGHT	SHEET: 1/1	

CARRIER ARM SCHEMATIC

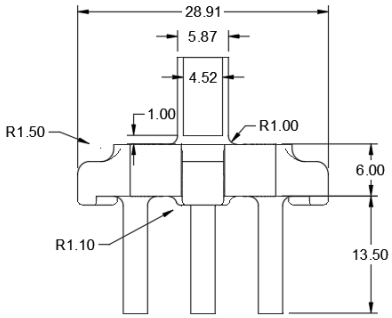

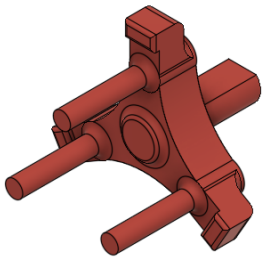

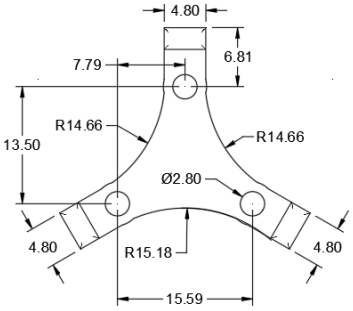

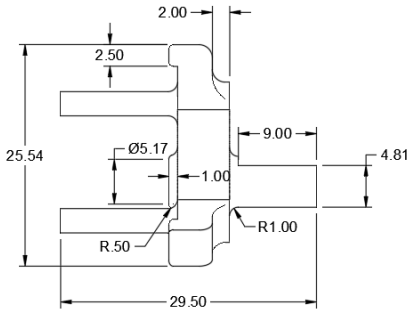

DIMENSIONS ARE IN MM TOLERANCE: ± 0.025 MM	PROJECT SEA Elbow Exoskeleton			
	TITLE Carrier Arm			
APPROVED	SIZE B	CODE	DWG NO Carrier_Arm_V10	REV 10
CHECKED				
DRAWN Benjamin Jenks 4/12/2024	SCALE 2.5:1	WEIGHT	SHEET 1/1	

COMPLIANT ARM DRAWING

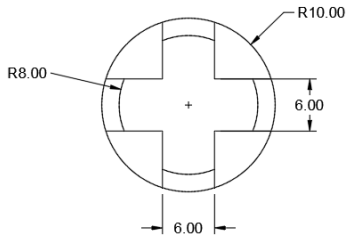

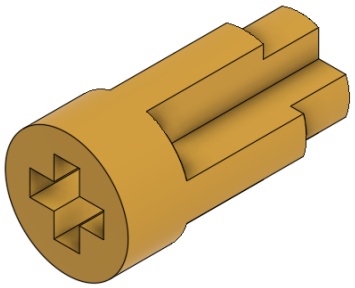

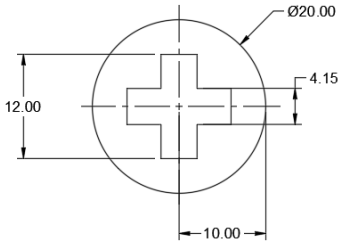

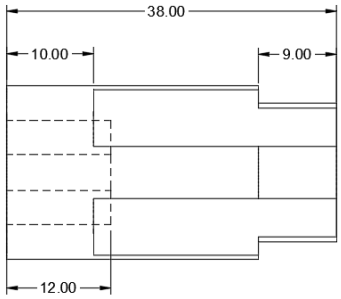

DIMENSIONS ARE IN MM TOLERANCE: ± 0.025 MM	PROJECT SEA Elbow Exoskeleton			
	TITLE Compliant Arm			
APPROVED	SIZE	CODE	DWG NO	REV
CHECKED	B		Compliant_Arm_V3	3
DRAWN Benjamin Jenks 4/12/2024	SCALE 2.5:1	WEIGHT	SHEET 1/1	

COUPLER SCHEMATIC

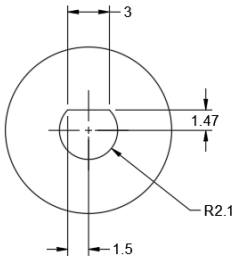

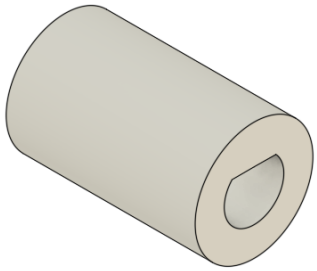

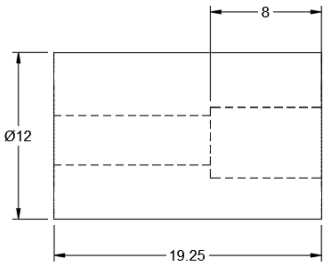

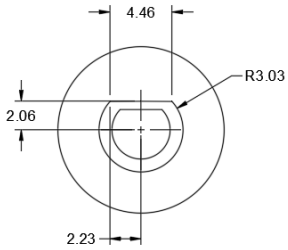

DIMENSIONS ARE IN MM TOLERANCE: ± 0.025 MM	PROJECT SEA Elbow Exoskeleton			
	TITLE Coupler			
APPROVED	SIZE	CODE	DWG NO	REV
CHECKED	B		Coupler_V9	9
DRAWN Benjamin Jenks 4/12/2024	SCALE 3:1	WEIGHT	SHEET 1/1	

FOREARM SCHEMATIC

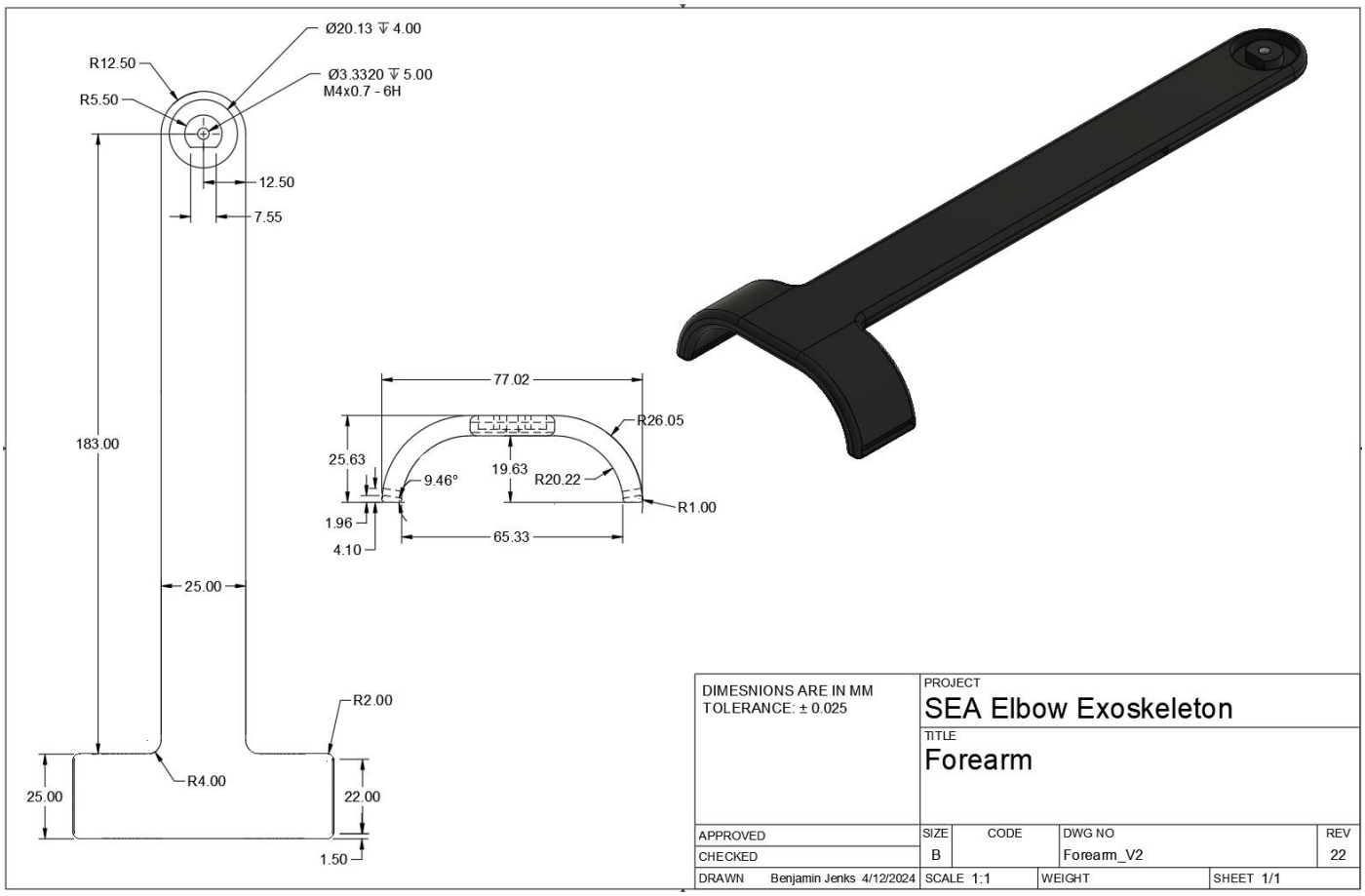

MOTOR BEVEL COMPLIANT SCHEMATIC

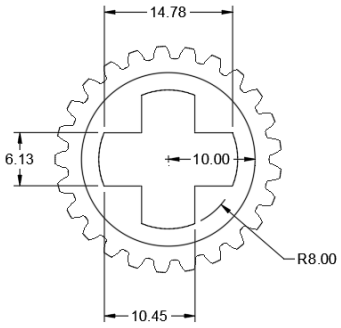

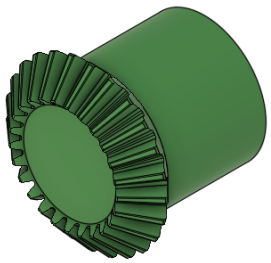

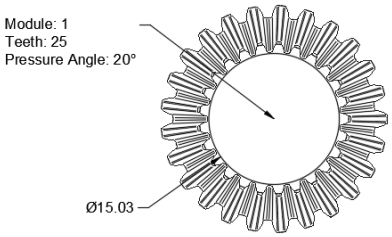

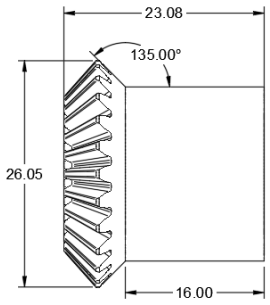

DIMENSIONS ARE IN MM TOLERANCE: ± 0.05 MM	PROJECT SEA Elbow Exoskeleton			
	TITLE Motor Bevel Compliant			
APPROVED	SIZE	CODE	DWG NO	REV
CHECKED	B		Motor_Bevel_Compliant_V3	3
DRAWN Benjamin Jenks 4/12/2024	SCALE 2.5:1	WEIGHT	SHEET 1/1	

MOTOR BEVEL SCHEMATIC

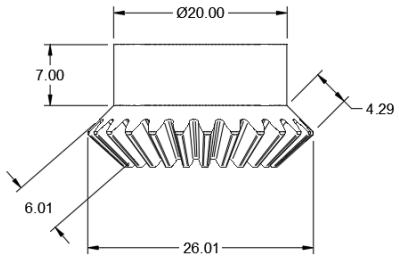

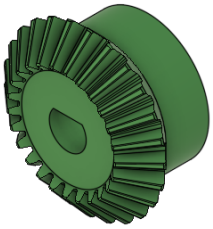

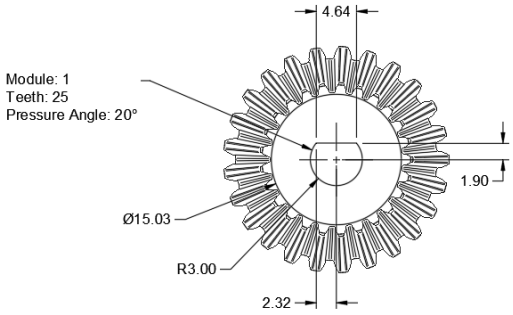

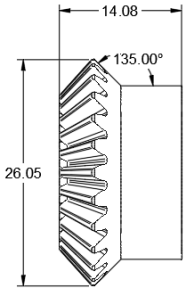

DIMENSIONS ARE IN MM TOLERANCE: ± 0.025 MM	PROJECT SEA Elbow Exoskeleton			
	TITLE Motor Bevel			
APPROVED	SIZE	CODE	DWG NO	REV
CHECKED	B		Motor_Bevel_V7	7
DRAWN Benjamin Jenks 4/12/2024	SCALE 2.5:1	WEIGHT	SHEET 1/1	

MOTOR BRACKET SCHEMATIC

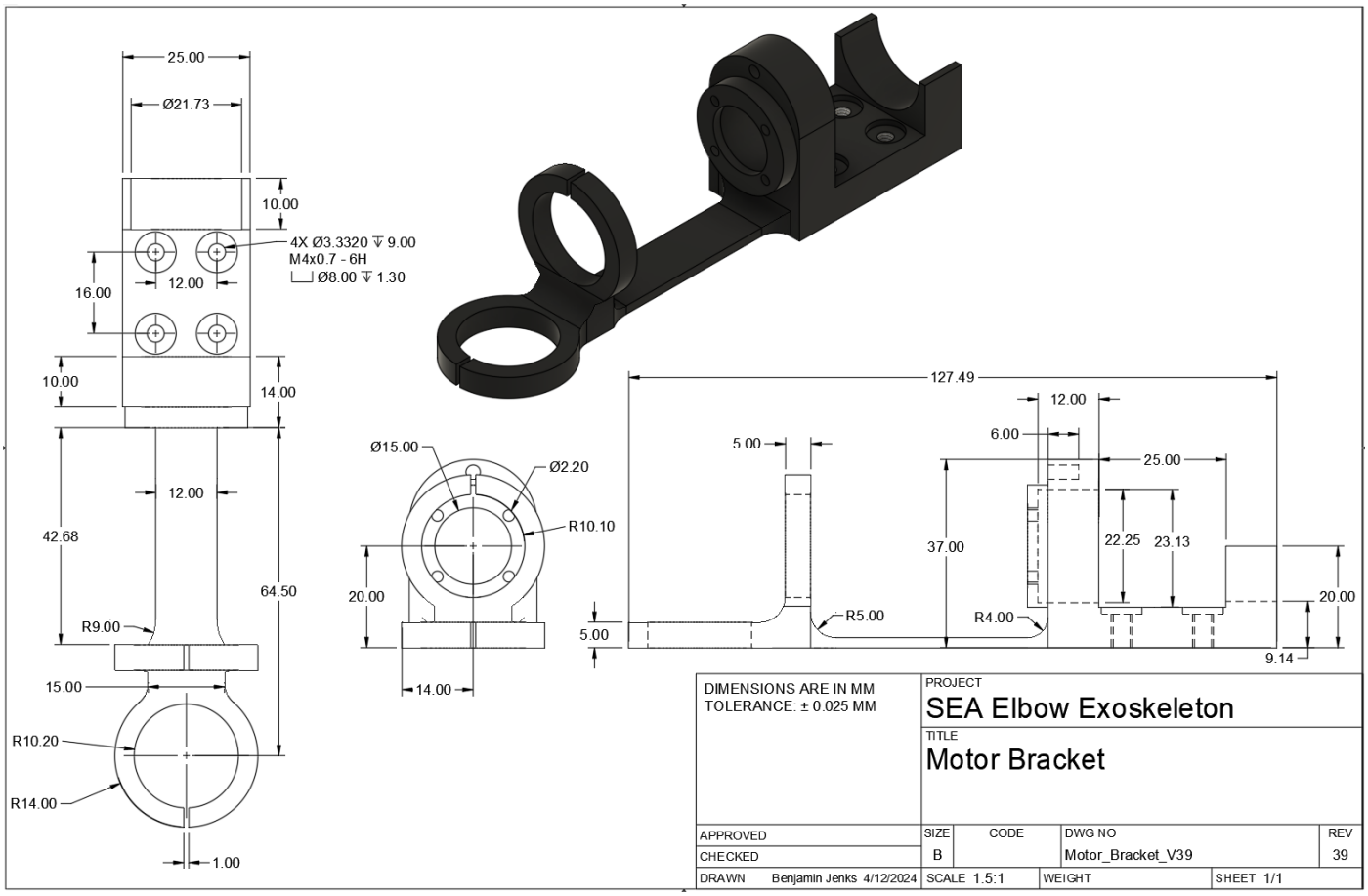

PLANET GEAR SCHEMATIC

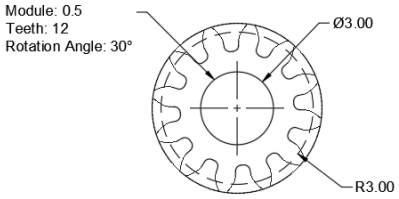

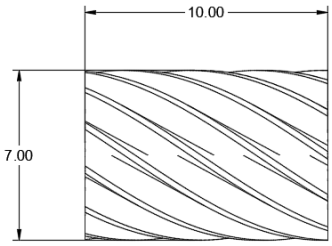

DIMENSIONS ARE IN MM TOLERANCE: ± 0.025 MM	PROJECT SEA Elbow Exoskeleton			
	TITLE Planet Gear			
APPROVED	SIZE B	CODE	DWG NO Planet_Gear_V10	REV 10
CHECKED				
DRAWN Benjamin Jenks 4/12/2024	SCALE 6:1	WEIGHT	SHEET 1/1	

PLANET STOP SCHEMATIC

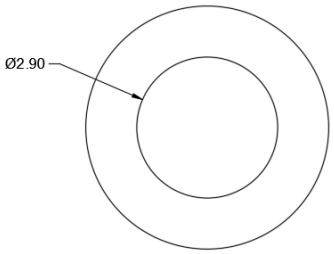

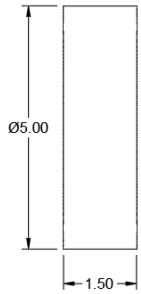

DIMENSIONS ARE IN MM TOLERANCE: ± 0.025 MM	PROJECT SEA Elbow Exoskeleton			
	TITLE Planet Stops			
APPROVED	SIZE	CODE	DWG NO	REV
CHECKED	B		Planet_Stops_V10	10
DRAWN Benjamin Jenks 4/12/2024	SCALE 14:1	WEIGHT	SHEET 1/1	

PLUS COUPLER SCHEMATIC

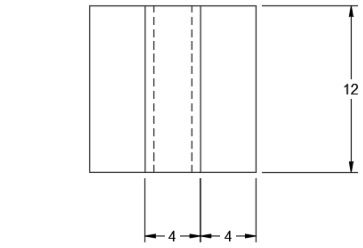

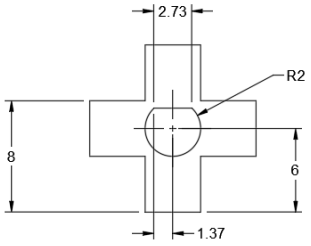

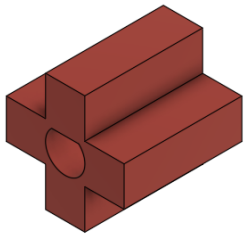

DIMENSIONS ARE IN MM TOLERANCE: ± 0.05 MM	PROJECT SEA Elbow Exoskeleton			
	TITLE Plus Coupler			
APPROVED	SIZE B	CODE	DWG NO Plus_Coupler_V6	REV 6
CHECKED				
DRAWN Benjamin Jenks 4/12/2024	SCALE 4:1	WEIGHT	SHEET 1/1	

RING GEAR SCHEMATIC

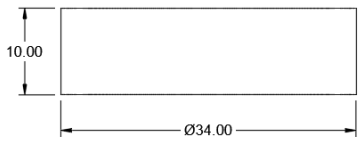

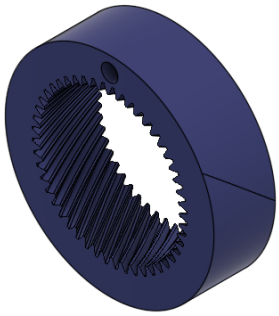

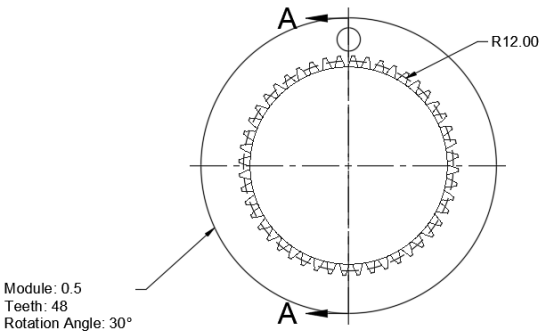

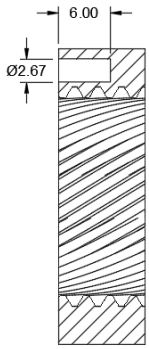

SECTION A-A
SCALE 2.5:1

DIMENSIONS ARE IN MM TOLERANCE: ± 0.025 MM	PROJECT SEA Elbow Exoskeleton			
	TITLE Ring Gear			
APPROVED	SIZE B	CODE	DWG NO Ring_Gear_V10	REV 10
CHECKED				
DRAWN Benjamin Jenks 4/12/2024	SCALE 2.5:1	WEIGHT	SHEET 1/1	

SUN GEAR SCHEMATIC

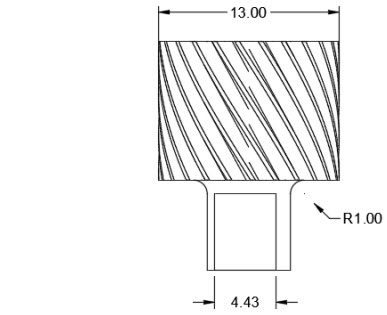

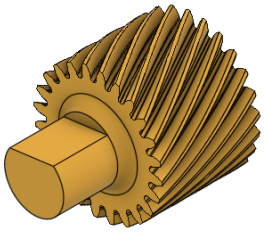

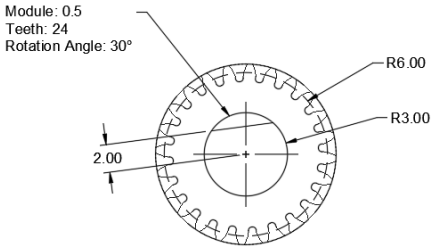

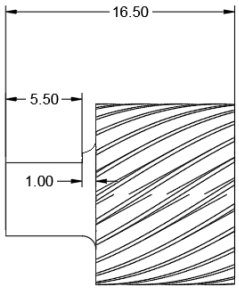

DIMENSIONS ARE IN MM TOLERANCE: ± 0.025 MM	PROJECT SEA Elbow Exoskeleton			
	TITLE Sun Gear			
APPROVED	SIZE B	CODE	DWG NO Sun_Gear_V10	REV 10
CHECKED				
DRAWN Benjamin Jenks 4/12/2024	SCALE 4:1	WEIGHT	SHEET 1/1	